Electronic Shell Effects in Fission Barriers and Fission Dynamics of Metal Clusters

We comment on various theoretical approaches currently used in investigations of metal-cluster fission, ranging from *ab initio* molecular-dynamics simulations to adaptation of phenomenological models developed in the context of nuclear fission and decay phenomena. By drawing analogies, as well as differences, between nuclear fission and nuclear radioactivity, and metal-cluster fission processes, we provide a unifying framework for investigations into the physical principles underlying modes of cluster fission, focusing on electronic shell effects and their importance in determining barriers and dynamical characteristics of cluster fission processes.

Key Words: *metal clusters, fission, shell effects, Born–Oppenheimer–LSD molecular dynamics, asymmetric two-center-oscillator shell model*

Fragmentation and fission processes underlie physical and chemical phenomena in a variety of systems, characterized by a wide spectrum of energy scales, nature of interactions, and characteristic spatial and temporal scales. These include nuclear fission,[1,2] fragmentation, unimolecular decay and reactions in atomic and molecular systems,[3] and more recently fission of atomic and molecular clusters.[4–11] Investigations of energetics, mechanisms, pathways, and stability, excitations, and dynamics of fission processes provide ways and means for exploring structure, stability, excitations and dynamics in multi-body (finite) systems, as well as allowing for comprehensive tests of theoretical methodologies and

Comments At. Mol. Phys.
1995, Vol. 31, Nos. 3–6, pp. 445–460
Reprints available directly from the publisher
Photocopying permitted by license only

conceptual developments, and have formed active areas of fruitful research endeavors in nuclear physics, and more recently in cluster science. Therefore, we focus our discussion on recent trends in studies of fission processes in metal clusters, and comment on issues pertaining to analogies and differences between such processes and those encountered in nuclear systems.

Multiply charged metallic clusters (M_n^{x+}) are observable in mass spectra if they exceed a critical size of stability n_c^{x+} (e.g., for $x = 2$, $n_c^{2+} = 27$ for Na and $n_c^{2+} = 19$ for K[4]). For clusters with $n > n_c^{x+}$, evaporation of neutral species is the preferred dissociation channel, while, below the critical size, fission into two charged fragments dominates (for $x = 2$, two singly charged fragments emerge). Nevertheless, at low enough temperature, such M_n^{x+} ($n < n_c^{x+}$) clusters can be metastable above a certain size n_b^{x+}, because of the existence of a fission barrier E_b (for Na_n^{2+} and K_n^{2+}, $n_b^{2+} = 7$[7,8]).

These observations indicate that fission of metal clusters occurs when the repulsive Coulomb forces due to the accumulation of the excess charges overcome the electronic binding (cohesion) of the cluster. This reminds us immediately of the well-studied nuclear fission phenomenon and the celebrated Liquid Drop Model (LDM)[1,2,12–15] according to which the binding nuclear forces are expressed as a sum of volume and surface terms, and the balance between the Coulomb repulsion and the increase in surface area upon volume conserving deformations allows for an estimate of the stability and fissility of the nucleus.[14,15]

Before discussing the LDM (and variants thereof), and its adaptability to the description of cluster fission, we note that for atomic and molecular clusters, microscopic descriptions of energetics and dynamics of fission processes, based on modern electronic structure calculations in conjunction with molecular dynamics (MD) simulations (where the classical trajectories of the ions, moving on the concurrently calculated electronic potential energy surface, are obtained via integration of the Newtonian equations of motion), are possible and have been performed.[7,8] Such calculations, using

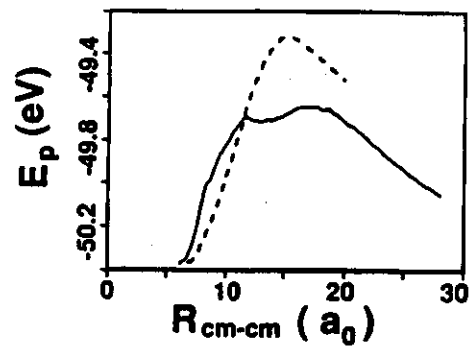

FIGURE 1 Molecular-dynamics results for the potential energy vs distance (in atomic units) between the centers of mass for the fragmentation of Na_{10}^{2+} into Na_7^+ and Na_3^+ (solid) and Na_9^+ and Na^+ (dashed), obtained via constrained minimization of the LSD ground-state energy of the system (Ref. 7).

norm-conserving nonlocal pseudopotentials and self-consistent solutions of the Kohn–Sham local spin-density functional (LSD) equations,[7,8,16] applied to small sodium[7] and potassium[8] clusters revealed several important trends (Figs. 1–3): (i) The energetically favorable fission channel for such doubly charged clusters is the asymmetric one, $M_n^{2+} \rightarrow M_{n-3}^+ + M_3^+$, containing a "magic" daughter M_3^+ (M = Na, K), i.e., $\Delta_m = E(M_{n-m}^+) + E(M_m^+) - E(M_n^{2+})$ is smallest for $m = 3$. (ii) Fission of clusters with $n \geq n_b^{2+}$, where $n_b^{2+} = 7$, involves barriers, whose magnitudes reflect the closed-shell stability of the parent cluster (i.e., E_b for $n = 10$ is particularly high), exhibiting a double-hump barrier shape (see Figs. 1 and 3a). (iii) The eventual fission products may already be distinguishable at a rather early stage of the fission process (on the top of the exit barrier for Na_{10}^{2+} (see Fig. 2) or prior to the exit barrier for K_{12}^{2+} (see Fig. 3), and the electronic binding between the two fragments is long-range in nature. (iv) The kinetic energy release $\mathcal{E}_r$ in the favorable channel obtained via dynamic simulations was found to be given by $\mathcal{E}_r \approx E_b + |\Delta_3|$, and the results correspond to experimental measurements[8] for K_n^{2+} ($5 \leq n \leq 12$). Furthermore, in agreement with experimental findings, the emerging fragments are

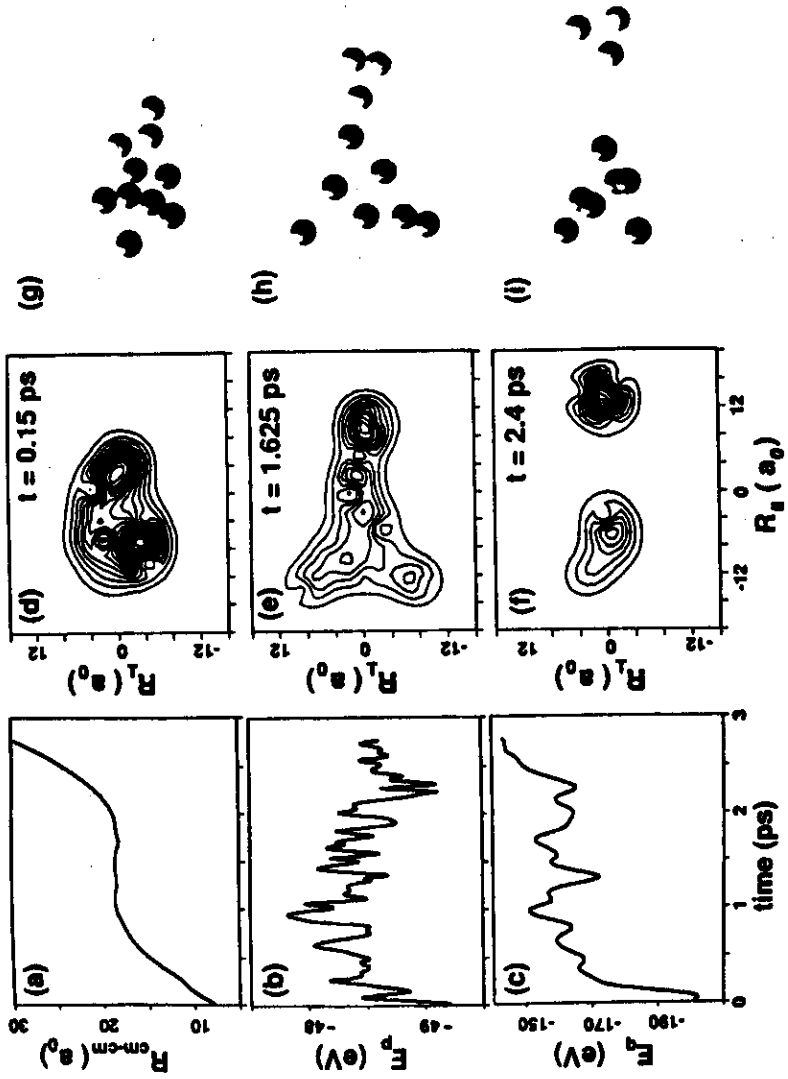

FIGURE 2 Fragmentation dynamics of Na_{10}^{2+} from first-principles Born–Oppenheimer local-spin-density functional molecular-dynamics simulations (Ref. 7). (a)–(c) Center-of-mass distance between the eventual fission products ($R_{c.m.-c.m.}$), total potential energy (E_p), and the electronic contribution E_q to E_p, vs time. (d)–(f) Contours of the total electronic charge distribution at selected times calculated in the plane containing the two centers of mass. The $R_\parallel$ axis is parallel to $R_{c.m.-c.m.}$. (g)–(i) Cluster configurations for the times given in (d)–(f). Dark and light balls represent ions in the large and small fragments, respectively. Energy, distance, and time in units of eV, bohr (a_0), and ps, respectively.

vibrationally excited, with the heating of the internal nuclear degrees of freedom of the fission products in the exit channel originating from dynamical conversion of potential into internal kinetic energy (see K_{9+}^{int} in Fig. 3b).

Several of the trends exhibited by the microscopic calculations (such as influence of magic numbers, associated with electronic shell closing, on fission energetics and barrier heights; predominance of an asymmetric fission channel; double-hump fission-barrier shapes; shapes of deforming clusters along the fission trajectory portraying two fragments connected through a stretching neck) suggest that appropriate adaptation of methodologies developed originally in the context of nuclear fission may provide a useful conceptual and calculational framework for studies of systematics and patterns of fission processes in metallic clusters.

We comment first on the earliest treatments of pertinent nuclear processes, i.e., fission[1,14] and alpha radioactivity.[2,17,18] Adaptation of the simple one-center LDM to charged metallic clusters,[9] involving calculation of the Coulomb repulsive energy due to an excess charge localized at the surface, yields a reduced LDM fissility parameter $\xi = (x^2/n)/(x^2/n)_{cr}$, where $(x_2/n)_{cr} = 16\pi r_s^3\sigma/e^2$ with the surface energy per unit area denoted by σ [using bulk r_s and σ values, $(x^2/n)_{cr} = 0.44$ and 0.39 for K_n^{x+} and Na_n^{x+}, respectively]. Accordingly, a cluster is unstable for $\xi > 1$ (implying that for K_n^{2+} with $n \leq 9$ and Na_n^{2+} with $n \leq 10$, barrierless fission should occur), with the most favorable channel being the symmetric one (i.e., when the two fragments have equal masses, which is only approximately true for nuclear fission, and certainly not the case for small metal clusters). For $0.351 < \xi < 1$, the system is metast-

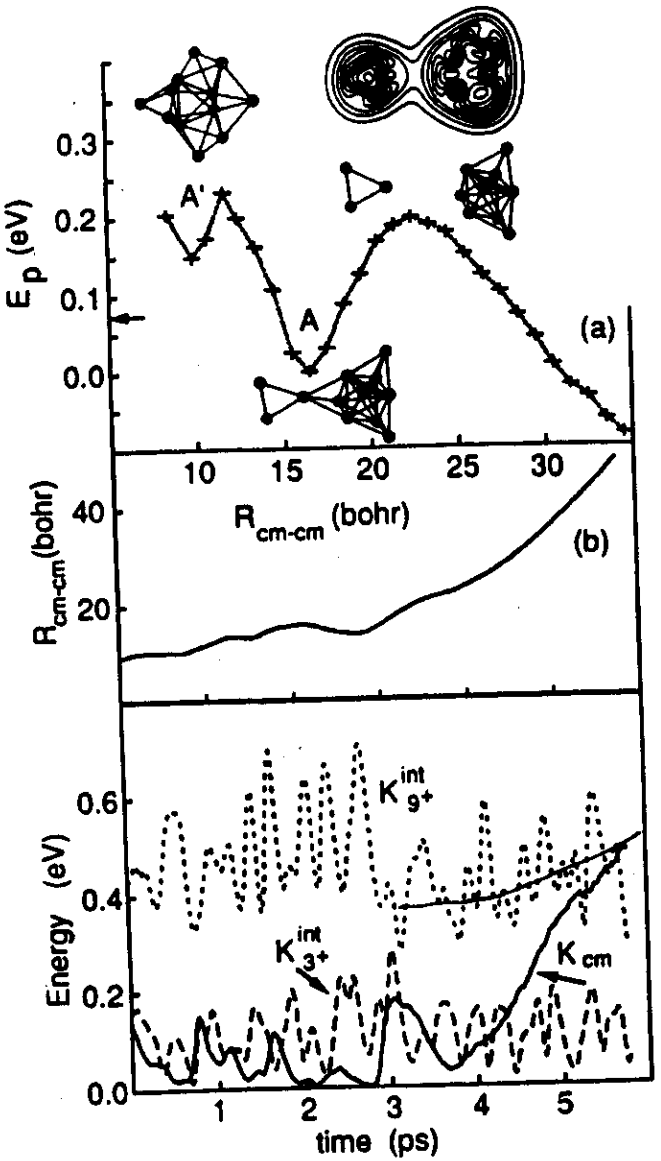

able (i.e., may fission in a process involving a barrier), and for $0 < \xi < 0.351$ the system is stable.

At the other limit, α-radioactivity, which may be viewed as an extreme case of (superasymmetric) fission, is commonly described as a process where the fragments are formed (or as often said, preformed) before the system reaches the top of the barrier (saddle point), and as a result the barrier is mainly Coulombic.[2] We note here that asymmetric emission of heavier nuclei is also known (e.g., $^{223}Ra \rightarrow {}^{14}C + {}^{209}Pb$, referred to as exotic or cluster radioactivity[19–21]), and the barriers in these cases resemble the one-hump barrier of alpha radioactivity and do not exhibit modulations due to shell effects.[21] We also remark that such α-radioactivity-type (essentially Coulombic) barriers have been proposed recently[10] for describing the overall shape of the fission barriers in the case of metal clusters.

Although several aspects of the simple LDM (e.g., competition between Coulomb and surface terms) and the α-particle Coulombic model (e.g., asymmetric channels and a scission configuration close to the location of the saddle of the multi-dimensional potential-energy surface) are present in the fission of metal clusters, neither model is adequate in light of the characteristic behavior revealed by the microscopic calculations and experiments discussed earlier. Rather, we find that proper treatments of fission in these systems require consideration of shell effects (for a recent experimental study that demonstrates the importance of shell effects

FIGURE 3 (a) Potential energy of K_{12}^{2+} fissioning in the favorable channel ($K_3^+ + K_9^+$) versus the interfragment distance $R_{c.m.-c.m.}$ obtained via constrained minimization. The origin of the E_p scale is set at the optimal prebarrier configuration (A). For large $R_{c.m.-c.m.}$, $E_p = -0.9$ eV, i.e., Δ_3. Included also are cluster configurations of K_{12}^{2+} corresponding to: a compact isomer (A') (the energy of the optimal compact isomer found is denoted by an arrow); the optimal bound configuration (A); the structure on top of the exit-channel barrier for which contours of the total electronic charge density, ρ, are shown (Ref. 8). (b) Time evolution of $R_{c.m.-c.m.}$, the internal vibrational kinetic energies of the fragments (K^{int}_{3+} and K^{int}_{9+}) and the sum of the fragments translational kinetic energies (K_{cm}) obtained via a BO-LSD-MD simulation starting from ionization ($t = 0$) of a K_{12}^+ cluster at 500 K. A line is drawn in K^{int}_{9+} for $t \geq 3$ ps) to guide the eye, illustrating heating of the internal vibrational degrees of freedom of the departing fragment.

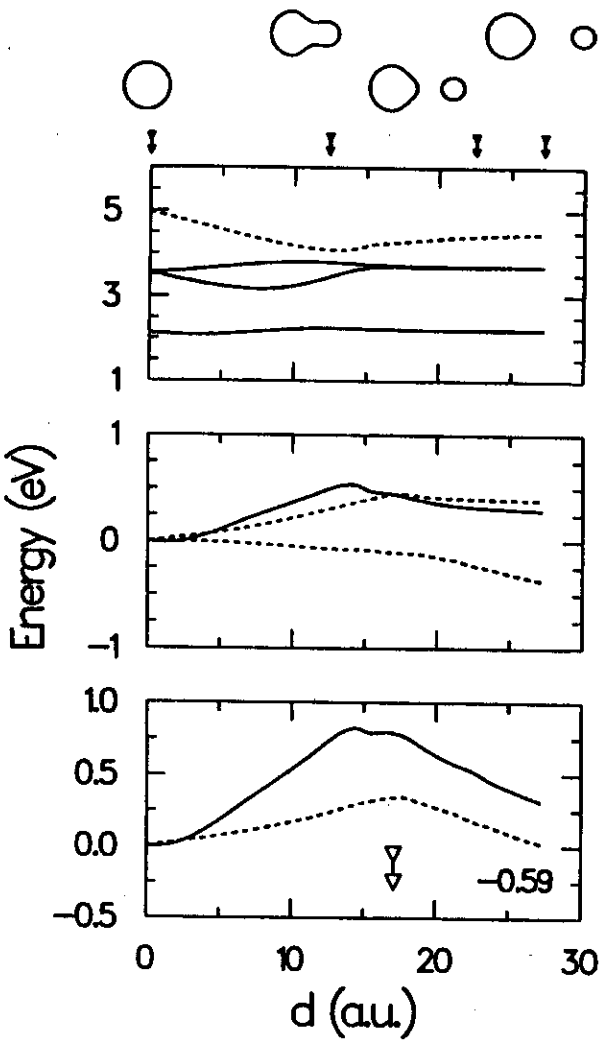

in metal-cluster fission, see Ref. 4b). While such effects are known to have important consequences in nuclear fission (transforming the one-hump LDM barrier for symmetric fission into a two-hump barrier,[2,22]), their role in the case of metal clusters goes even further. Indeed, as illustrated below for the case of the magic Na_{10}^{2+}, shell effects can be the largest contribution to the fission barrier, even in instances when the LDM component exhibits no barrier (in this case the LDM fissility $\xi > 1$). In this respect, Na_{10}^{2+} is analogous to the case of superheavy nuclei, which are believed[23] to be stabilized by the shell structure of a major shell closure at $Z = 114$, $N = 184$ (Z is the number of protons and N is the number of neutrons; unfortunately such nuclei have not yet been observed or synthesized artificially). Equally important is our observation that incorporation of shell effects in models of fission of metal clusters requires a description at the level of an asymmetric two-center-oscillator shell model[24] (ATCOSM), due to the influence of the shell effects of the fragments upon the barrier heights, unlike the nuclear case where oscillations in the single-particle level density of the parent, as a function of the degree of deformation of the nucleus, calculated with one-center shell models (e.g., the Nilsson model), are often sufficient to yield double-hump barriers.[2]

In the calculations, whose results we present below, we have adapted the ATCOSM, developed[21] with the aim of unifying treatments of fission, alpha, and exotic radioactivity, in conjunction with an averaging procedure of the single-particle spectra[25] based

FIGURE 4 ATCOSM results for the superasymmetric channel $Na_{10}^{2+} \rightarrow Na_9^+ + Na^+$. The parent (in the initial configuration) and both fragments (in the final configurations) are spherical. Bottom panel: LDM energy (surface plus Coulomb, dashed curve) and total potential energy (LDM plus shell corrections, solid curve) as a function of fragment separation d. The empty vertical arrow marks the scission point. The displayed number (−0.59 eV) denotes the dissociation energy $\Delta_1 = E(Na_9^+) + E(Na^+) - E(Na_{10}^{2+})$, which defines the limiting value of the total energy (solid curve) at infinite separation. Middle panel: Shell-correction contribution (solid curve), surface contribution (upper dashed curve), and Coulomb contribution (lower dashed curve) to the total energy, as a function of fragment separation d. Top panel: Single-particle spectra as a function of fragment separation d. The occupied levels are denoted by solid lines. The unoccupied levels are denoted by dashed lines. On top of the figure, four snapshots of the evolving cluster shapes are displayed. The solid vertical arrows mark the corresponding fragment separations.

on an $\hbar$-expansion of the semiclassical partition function introduced by Wigner and Kirkwood.[26] Consequently, the shell correction, Δ_{sh}, is given by

$$\Delta_{sh} = \sum_{i}^{occ} \varepsilon_i - \tilde{E},$$

where ε_i are the single-particle levels of the asymmetric two-center-oscillator Hamiltonian, and $\tilde{E}$ is the average energy of the single-particle spectrum (we mention here that shell corrections, in the context of unification of the liquid drop and the independent-particle models, were introduced in nuclear physics by Strutinsky[27]; for a discussion of shell corrections, including an averaging procedure in the context of LDA calculations for metal clusters, see Ref. 28(a). For an application of shell corrections to triaxially deformed clusters, see Ref. 28(b).

We also note that the ATCOSM which we used (including a fourth-order expression for the neck potential[29]) provides a proper four-parameter description going beyond the three-parameter model which was recently employed.[11] The restrictions imposed by the latter model[11] on the deformation degrees of freedom, together with the cavity model of the cluster used (namely, imposing a boundary condition of vanishing wave functions at the metal-cluster surface, thus not allowing for electronic spill-out), led to exaggerated shell effects which do not saturate after the scission point, resulting in asymptotic fission products which are not in their ground state.

Results[30] of the ATCOSM for two fission channels of Na_{10}^{2+}, (i) $Na_9^+ + Na^+$ and (ii) $Na_5^+ + Na_5^+$, illustrating fission characteristics in the supersymmetric (SA) and symmetric (S) fission limits, are shown in Figs. 4 and 5. The SA channel—with a mass asymmetry $\eta = 1/9$, compared to $\eta = 4/(A-4) << 1$ (typically $1/50 - 1/60$; $A = N + Z$ is the nuclear mass number) for α-decay in nuclei—exhibits relatively mild variations of the single-particle levels along the fission coordinate, a single-hump barrier composed, almost equally, of

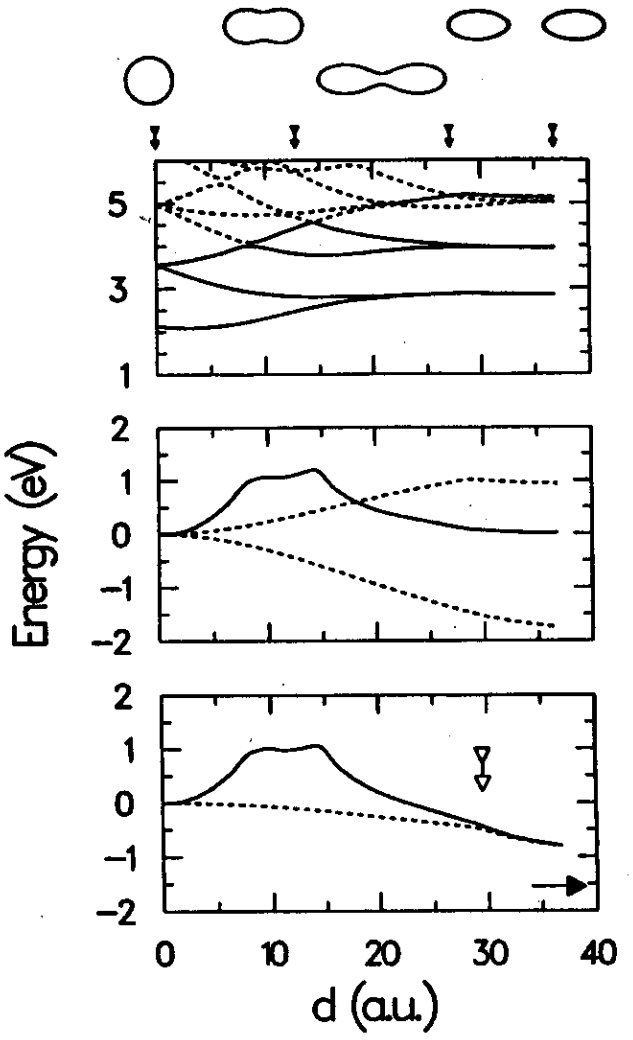

FIGURE 5 ATCOSM results for the symmetric channel $Na_{10}^{2+} \rightarrow Na_5^+ + Na_5^+$. Both fragments are prolate in their final configurations with a ratio of shorter-axis/longer-axis = 0.50. Panel distribution and other notations are the same as in Fig. 4. The horizontal solid arrow marks the dissociation energy Δ_S.

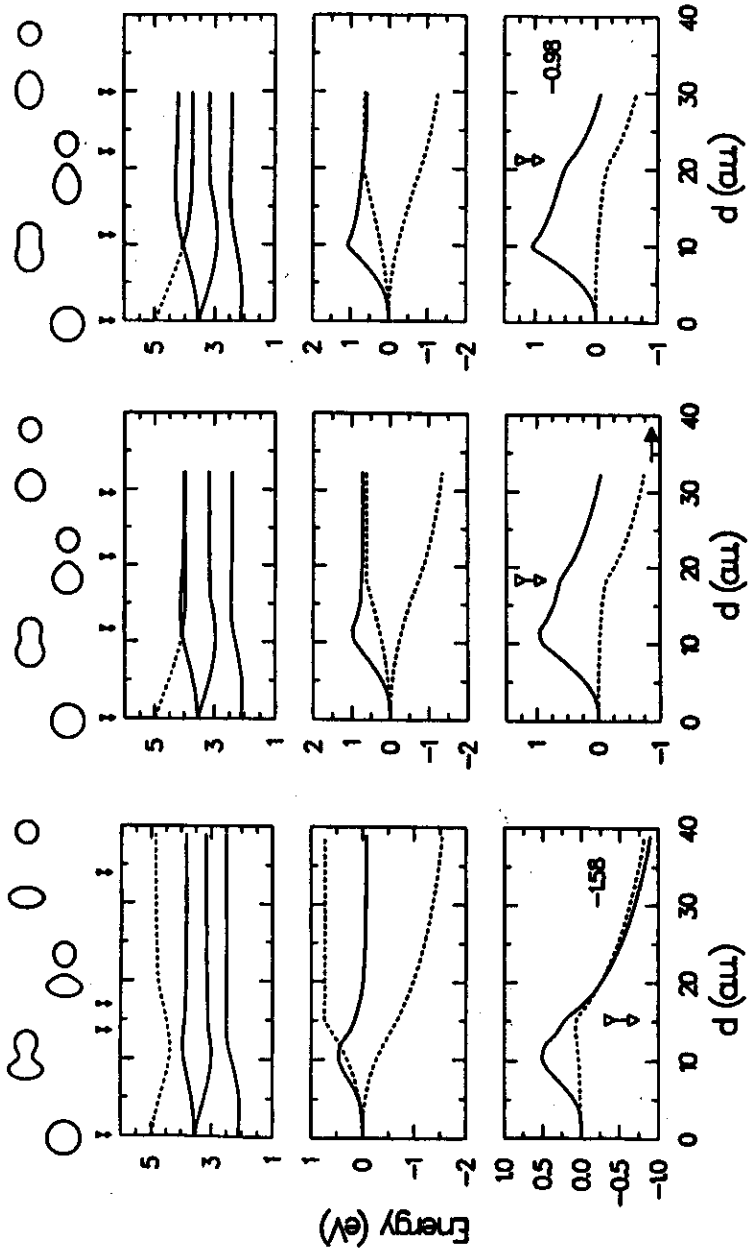

LDM and shell-correction contributions, and scission close to the top of the barrier, characteristic of a fission process involving "preformation" (consequently, the corresponding shell contributions are attributed to the assignment of the eight electrons from the original volume of Na_{10}^{2+} to the slightly smaller volume of Na_9^+). In contrast, the symmetric channel ($\eta = 1$) is characterized by single-particle level splitting and crossing, a double-hump barrier originating solely from shell-structure contributions, and a scission point far from the top of the barrier (thus suggesting that not only the deformed fragments, but also the deformation degree of the parent participates significantly in the shell effect).

In Fig. 6, we show fission characteristics in the energetically most favorable channel ($Na_7^+ + Na_3^+$), calculated for three configurations (shapes) of the emerging fragments (o,s), (s,s), and (p,s), where (a,b) designates the shapes of the heavy and light fragments, and o, s, and p denote oblate, spherical, and prolate shapes. Both our model and microscopic LSD[7] calculations show that (o,s) is the energetically preferred configuration in this channel. These results illustrate the dependence of the fission characteristics along the fission trajectory (single-particle spectral variations, LDM and shell-correction contributions, barrier shapes and heights) on the shapes and relative orientations of the emerging fragments, indicating again that shell corrections associated with the fragments make a significant contribution to the fission energetics and barriers.

In this brief exposition, we hope we have elucidated certain issues pertaining to fission processes of metallic clusters, focusing

FIGURE 6 ATCOSM results for the asymmetric channel $Na_{10}^{2+} \rightarrow Na_7^+ + Na_3^+$. The final configuration of Na_3^+ is spherical. For the heavier fragment Na_7^+, we present results associated with three different final shape configurations, namely, oblate [(o,s); left], spherical [(s,s); middle], and prolate [(p,s); right]. The ratio of shorter to longer axis is 0.555 for the oblate case and 0.75 for the prolate case. Panel distribution and other notations are the same as in Fig. 4. A number (–1.58 eV or –0.98 eV), or a horizontal solid arrow, in a lower panel denotes the corresponding dissociation energy Δ_3. Notice the change in energy scale for the middle and bottom panels, as one passes from (o,s) to (s,s) and (p,s) final configurations.

on electronic shell effects and their importance in determining the energetics, structure, pathways, and dynamical mechanisms of fission in these systems, and have outlined and demonstrated various theoretical approaches currently used in investigations of cluster fission, ranging from microscopic first-principles electronic structure calculations coupled with molecular dynamics simulations to adaptation of models more phenomenological in nature originated in studies of nuclear fission. By drawing analogies, as well as differences, between certain aspects of nuclear fission and nuclear radioactivity phenomena and atomic (metallic) cluster fission processes, we have attempted to provide a unifying conceptual framework for discussing the physical principles underlying modes of cluster fission (i.e., shell effects originating from fragments and parent, asymmetric and symmetric fission, single- and double-hump barriers, fissioning cluster shapes, and dynamical aspects, such as the time scale of fission processes, kinetic energy release, and dynamical energy redistribution among the fission products).

We conclude by commenting on some experimental and theoretical issues in cluster fission which remain as future challenges (limiting ourselves to metallic clusters). These include: fission dynamics of multiply charged large metal clusters[6,31]; systematic investigations of temperature effects on modes of cluster fission, and ternary and higher multi-fragmentation processes; time-resolved spectroscopy of fission processes and fission isomers; spin effects in fission; tunneling processes and corresponding lifetimes in subbarrier fission modes of clusters of light elements, e.g., lithium; and fission processes of nonsimple metal clusters.

Acknowledgment

This research was supported by a grant from the U.S. Department of Energy (Grant No. AG05-86ER45234).

C. YANNOULEAS, R. N. BARNETT and UZI LANDMAN

School of Physics,
Georgia Institute of Technology,
Atlanta, Georgia 30332-0430

References

1. A. Bohr and B. R. Mottelson, *Nuclear Structure* (Benjamin, Reading, MA, 1975), Vol. II.
2. M. A. Preston and R. K. Bhaduri, *Structure of the Nucleus* (Addison-Wesley, London, 1975).
3. W. Frost, *Theory of Unimolecular Reactions* (Academic, New York, 1973); see also D. Scharf, U. Landman and J. Jortner, Chem. Phys. Lett. **126**, 495 (1986); D. Scharf, J. Jortner and U. Landman, J. Chem. Phys. **88**, 4273 (1988); H.-P. Kaukonen, C. L. Cleveland and U. Landman, J. Chem. Phys. **95**, 4997 (1991); R. Schmidt, G. Seifert and H. O. Lutz, Phys. Lett. **A158**, 231 (1991).
4. (a) C. Bréchignac, Ph. Cahuzac, F. Carlier and M. de Frutos, Phys. Rev. Lett. **64**, 2893 (1990); C. Bréchignac, Ph. Cahuzac, F. Carlier, J. Leygnier and A. Sarfati, Phys. Rev. B **44**, 11386 (1991); (b) C. Bréchignac *et al.*, Phys. Rev. B **49**, 2825 (1994).
5. W. A. Saunders, Phys. Rev. Lett. **64**, 3046 (1990); *ibid.* **66**, 840 (1991).
6. T. P. Martin, U. Näher, H. Göhlich and T. Lange, Chem. Phys. Lett. **196**, 113 (1992); U. Näher, H. Göhlich, T. Lange and T. P. Martin, Phys. Rev. Lett. **68**, 3416 (1992).
7. R. N. Barnett, U. Landman and G. Rajagopal, Phys. Rev. Lett. **67**, 3058 (1991); see also R. N. Barnett and U. Landman, Phys. Rev. Lett. **69**, 1472 (1992).
8. C. Bréchignac, Ph. Cahuzac, F. Carlier, M. de Frutos, R. N. Barnett and U. Landman, Phys. Rev. Lett. **72**, 1636 (1994).
9. W. A. Saunders, Phys. Rev. A **46**, 7028 (1992).
10. J. M. López, J. A. Alonso, F. Garcias and M. Barranco, Ann. Phys. (Leipzig) **1**, 270 (1992); F. Garcias, J. A. Alonso, J. M. López and M. Barranco, Phys. Rev. B **43**, 9459 (1991).
11. H. Koizumi, S. Sugano and Y. Ishii, Z. Phys. D **28**, 223 (1993); M. Nakamura, Y. Ishii, A. Tamura and S. Sugano, Phys. Rev. A **42**, 2267 (1990).
12. C. F. von Weizsäcker, Z. Phys. **96**, 431 (1935).
13. H. A. Bethe and R. F. Bacher, Rev. Mod. Phys. **8**, 82 (1936).
14. N. Bohr and J. A. Wheeler, Phys. Rev. **56**, 426 (1939).
15. J. R. Nix and W. J. Swiatecki, Nucl. Phys. **71**, 1 (1965).
16. For a detailed description of the Born–Oppenheimer local-spin-density functional molecular-dynamics (BO-LSD-MD) method, see R. N. Barnett and U. Landman, Phys. Rev. B **48**, 2081 (1993).
17. G. Gamow, Z. Phys. **51**, 204 (1928).
18. E. U. Condon and R. W. Gurney, Nature **122**, 439 (1928).
19. A. Sandulescu, D. N. Poenaru and W. Greiner, Sov. J. Part. Nucl. **11**, 528 (1980).
20. P B. Price, Ann. Rev. Nucl. Part. Sci. **39**, 19 (1989).
21. For a theoretical review, see W. Greiner, M. Ivascu, D. N. Poenaru and A. Sandulescu, "Cluster Radioactivities," in *Treatise on Heavy-Ion Science*, ed. D. A. Bromley (Plenum, New York, 1989), Vol. 8, p. 641.
22. S. G. Nilsson *et al.*, Nucl. Phys. A **131**, 1 (1969).
23. W. D. Myers and W. J. Swiatecki, Nucl. Phys. **81**, 1 (1966).
24. J. Maruhn and W. Greiner, Z. Phys. **251**, 431 (1972).
25. B. K. Jennings, R. K. Bhadhuri and M. Brack, Phys. Rev. Lett. **34**, 228 (1975).
26. E. P. Wigner, Phys. Rev. **40**, 749 (1932); J. G. Kirkwood, Phys. Rev. **44**, 31 (1933).
27. V. M. Strutinsky, Nucl. Phys. A **95**, 420 (1967); V. M. Strutinsky, Nucl. Phys. A **122**, 1 (1968).

28. (a) C. Yannouleas and U. Landman, Phys. Rev. B 48, 8376 (1993); C. Yannouleas and U. Landman, Chem. Phys. Lett. 210, 437 (1993); (b) C. Yannouleas and U. Landman, Phys. Rev. B 51, 1902 (1995).
29. M. G. Mustafa, U. Mosel and H. W. Schmitt, Phys. Rev. C 7, 1519 (1973).
30. For details of the ATCOSM applied to investigations of metal clusters, see C. Yannouleas and U. Landman, Phys. Rev. B (to be published).
31. C. Bréchignac, Ph. Cahuzac, F. Carlier and J. Leygnier, Phys. Rev. Lett. 63, 1368 (1989).